ICANS-VI

INTERNATIONAL COLLABORATION ON ADVANCED NEUTRON SOURCES

June 27 - July 2, 1982

MEASURED AND CALCULATED NEUTRON YIELDS FOR 100 MeV PROTONS ON THICK TARGETS OF Pb AND Li

by

R.T. Jones, M.A. Lone, A. Okazaki, B.M. Townes,
D.C. Santry and E.D. Earle
Atomic Energy of Canada Limited
Chalk River Nuclear Laboratories
Chalk River, Ontario K0J 1J0

J.K.P. Lee, J.M. Robson, R.B. Moore and V. Raut
McGill University
Montréal, Québec

ABSTRACT

The neutron yield per proton from thick targets of lead and lithium irradiated with 100 MeV protons has been measured and calculated. The water bath method was used to measure the neutron production, and a Faraday cup for the the beam current determination. Measured yields are 0.343 ± 0.021 for lead and 0.123 ± 0.007 for lithium. Corresponding yields calculated with the nucleon-meson transport code NMTC are 0.363 ± 0.002 and 0.160 ± 0.001. Measured and calculated thermal neutron distributions in the water bath are also compared.

June 1982

MEASURED AND CALCULATED NEUTRON YIELDS FOR 100 MeV PROTONS ON THICK TARGETS OF Pb and Li

R.T. Jones, M.A. Lone, A. Okazaki, B.M. Townes
D.C. Santry and E.D. Earle
Atomic Energy of Canada Limited
Chalk River Nuclear Laboratories
Chalk River, Ontario K0J 1J0

J.K.P. Lee, J.M. Robson, R.B. Moore and V. Raut
McGill University
Montréal, Québec

1. INTRODUCTION

AECL has a research and development program aimed at constructing an accelerator and neutron producing target for economic breeding of fissile material, the so-called Breeder Accelerator (BA)[1,2]. The planned stages of the program are:

(1) ZEBRA (Zero Energy BReeder Accelerator)

Beam: 300 mA protons at 10 MeV

Purpose: To gain understanding of accelerator operation at high current and low energy.

(2) EMTF (Electronuclear Materials Test Facility)

Beam: 70 mA protons at 200 MeV

Purpose: Further accelerator development and materials testing using neutrons from a Pb-Bi target.
Thermal neutron source for fundamental research. (Flux available $\sim 10^{15}$ n.cm^{-2}.s^{-1})

(3) PILOT BA

Beam: 70 mA protons at 1000 MeV

Purpose: Accelerator development and target blanket development at moderate power levels.

(4) DEMO BA

Beam: 300 mA protons at 1000 MeV

Purpose: Full scale demonstration of electro-nuclear breeding.

The work described here is to help with the design and performance assessment of the target for the EMTF. There are very few measurements of neutron yields from thick targets for protons with energies in the range 50 to 400 MeV. We have measured such yields from targets of lead and lithium for 100 MeV protons. These measurements will provide a benchmark for the computer codes used to design the EMTF target-moderator assembly. We also present results calculated using the codes NMTC and MORSE for the experimental geometry.

2. EXPERIMENTS

2.1 General Description

The 100 MeV proton beam of the McGill Cyclotron was used to irradiate thick targets of Pb (1.6 cm thick by 6.2 cm diameter) and Li enriched to 99.995 wt.% Li-7 (17.4 cm long by 5.7 cm diameter). A large tank of light water surrounding the targets thermalized and captured the neutrons produced and also served as part of the Faraday cup for proton current measurement. The neutron source strength was derived from measurements of the thermal neutron flux distribution in the water.

2.2 Beam Current Measurement

The beam line and target arrangement are shown in Figure 1. The remotely controlled quartz scintillator was used to initially align the

beam and to periodically monitor its alignment and profile during an irradiation. Continuous monitoring of the current on the 2.5 cm ID brass collimator also safeguarded against abrupt changes in beam profile or position and ensured that only the target was irradiated. Post-irradiation autoradiography of a lead target confirmed that the beam spot although not quite circular was only $\sim$1 cm in diameter.

To measure the integrated charge on the target, the target tube and the water tank were electrically connected and insulated from ground to form a large Faraday cup. This was connected to a low impedance, low noise current integrator. Extensive tests were performed to check the accuracy of the current integration.

The current integrator was calibrated with a precision current source which verified its accuracy to $\pm$0.1% on the 10^{-8} and 10^{-9} A ranges. A portable current source was used to measure the effect of the shunt impedance of the Faraday cup with no beam. This made less than 0.4% difference to measurements of currents of about 50 nA.

With the beam on, other systematic errors in the current measurement are possible. Ionization current in the residual gas in the target tube was calculated to be negligible due to the low pressure of the gas and the large length (75 cm) and small diameter (6.3 cm) of the tube. The geometry of the tube also helped to suppress the loss of secondary electrons from the Faraday cup as did permanent magnets placed near its outer end. Leakage of charge from the Faraday cup due to ionization in the target room was measured by stopping the beam upstream in a thick copper block. The beam was adjusted such that the measured radiation level in the target room was similar to that experienced in an actual irradiation. This test indicated a systematic error of less than 0.8%.

Radio frequency pick-up on the Faraday cup was negligible from the cyclotron but considerable from a nearby television transmitter. A π filter in the lead to the integrator reduced this effect by several orders

of magnitude. Residual current due to RF pick-up was of the order of 0.1 nA and was monitored during the irradiation by occasionally switching off the beam. The integrated charge was corrected for this effect which introduced an uncertainty of less than 0.2%. The filter circuit also provided protection against pulse saturation of the integrator due to the pulsed nature of the synchrocyclotron beam.

Typical average beam currents were about 50 nA with an estimated overall uncertainty of less than 1.5%.

2.3 Neutron Yield Measurement

The basis of the method is that the fate of the great majority of neutrons produced in the target is moderation followed by capture in the water bath. A measurement of the volume integrated thermal flux combined with the absorption cross section of water can therefore be equated with the neutron yield, provided the small corrections for leakage, fast neutron absorption, and thermal neutron absorption in other than water can be made.

To minimize leakage a large tank in the form of a vertical cylinder (1.7 m high by 1.5 m diameter) was used (Fig. 2). The back face of the targets was located about 60 cm from the front surface of the tank at its mid-height.

The method chosen to measure the neutron flux was activation of gold foils attached to a lucite frame in the vertical plane above the target tube. About 70 foils of thickness either 0.254 mm or 0.051 mm and diameter 11.3 mm were used, distributed as indicated in Fig. 2. This gives the spatial flux distribution which must be integrated. To minimize the number of foils used most measurements were made in the plane above the target tube. The frame was, however, equipped with arms below and to either side at the position immediately downstream from the target. These enabled azimuthal asymmetries in the flux distribution, due to non uniformities in the beam profile or radial displacement of the beam from the target centre,

to be measured. A correction for azimuthal variation was made to the measured fluxes before integration.

The gamma activity of the foils was counted on an automatic system with two NaI(Tl) detectors connected to counting channels biased at 50 keV. Preliminary data analysis corrected for counter dead time, room background and radioactive decay during and since the irradiation. The efficiency of the counter system for Au-198 activity had been previously established using standardized gold foils of the same diameter as those used here but of different thickness (0.025 mm). A correction for the different gamma-ray absorption in the present foils allowed their Au-198 activity content to be calculated.

To obtain the neutron flux from the activity the effective macroscopic absorption cross section for gold, $\hat{\Sigma}$, is required. We use the Westcott convention[3] to define this

$$\hat{\Sigma} = \hat{\Sigma}_o(GBg + G_r rs)$$

where Σ_o is the macroscopic cross section for 2200 $m \cdot s^{-1}$ neutrons (5.835 cm^{-1}), g and s are the Westcott cross section parameters [defined in (3)], and r is the Westcott epithermal flux index. G and B are factors accounting for thermal neutron flux depression in the foil and in the moderator around the foil, respectively. G_r is a similar quantity to G but for neutrons at the Au-197 resonance energy (4.9 eV).

The epithermal flux index, as a function of distance from the target, was obtained from an irradiation in which some of the foils were covered with cadmium. G_r was calculated from (4) and s taken from (5), the resulting correction for epi-cadmium activation was ~3.6% for 0.254 mm foils and ~6.4% for 0.051 mm foils. Values for the product GB were obtained from subsidiary experiments: GB = 0.715 for 0.254 mm foils and 0.923 for 0.051 mm foils.

3. RESULTS

The measured thermal flux distributions, normalized to a 1 mA proton current, are shown in Figs. 3 and 4. That for the lithium target is much less steeply sloped. This may be ascribed to a higher average neutron energy in the source spectrum and a spatially more distributed source. These fluxes have been corrected for azimuthal variation of the flux measured in the previously described manner. The largest of these corrections was about 10%. This occurred before alignment of the beam was finalized. With better beam alignment the corrections fell in the range 1% to 4%.

To integrate the flux over the measurement volume cubic splines were fitted to the logarithm of the flux. This was done first for the axial (z) distributions at each radius (r) where measurements had been made, then radially. The lines in Figs. 3 and 4 are the fitted splines. Because of the discontinuity in the measurement array caused by the target tube the integration was done for positive and negative z separately. The zero of the z co-ordinate is shown in Figs. 2 and 3.

Various checks were made on the accuracy of the integration method. These included reversing the order of integration (r then z), including measurements at extra radial positions for one irradiation and integrating over all z at once. The results showed systematic differences in the range $\pm$1%.

For the lithium target results it was necessary to extrapolate the fluxes beyond the measurement volume. An exponential extrapolation was used and increased the integral by $\sim$ 5%.

To obtain the neutron absorption rate in the water, the integrated flux is multiplied by the appropriate macroscopic absorption cross section (0.0220 cm^{-1} was used). This can be equated to the neutron source strength

if allowance is made for the small numbers of neutrons lost in other ways. These include thermal neutron absorptions in the target and target tube ($\ll$1% for both targets), absorption of non-thermal neutrons ($\sim$1.4% for Pb target, $\sim$1.9% for Li), and leakage of neutrons of all energies (0.3% for Pb target, 0.5% for Li). The first of these corrections was based on the measured thermal fluxes and known cross sections, the other two were derived from the calculations described in the next section.

The measured neutron yields for three irradiations with Pb targets and one with a Li-7 target are shown in Table 1. The uncertainty in the measurement, derived from the three results for lead, is $\pm$3%. A separate error analysis in which errors were assigned to each of the separate factors needed to derive the measured yield indicated an overall error of $\pm$6%. These estimates are in reasonable agreement since the first cannot detect some systematic effects which were included in the second.

4. CALCULATION OF NEUTRON YIELDS AND FLUXES AND COMPARISON WITH MEASURED VALUES

4.1 Method of Calculation

The calculations for these experiments were performed using a combination of computer codes and nuclear data which were originally set up for accelerator breeder target studies at CRNL.

The (p,n) production and neutron transport down to neutron energies below a 14.9 MeV cut-off energy were computed using NMTC[6], a nucleon-meson transport code. This code employs Monte Carlo techniques to provide a detailed description of the transport process using the intranuclear-cascade-evaporation model of nuclear interactions. The intranuclear-cascade calculation is based on Bertini's medium-energy

intranuclear-cascade code[7], and the evaporation calculation is carried out using a version of Guthrie's evaporation code[8]. Slowing down of charged particles due to excitation and ionization of atomic electrons is treated using the continuous slowing down approximation, and elastic collisions with all nuclei other than hydrogen are neglected. When the neutron energy falls below the 14.9 MeV cut-off its location, energy and direction are stored, and a random sample of these neutrons is used as an input source distribution for the MORSE[9,10] code, which tracks each neutron until it is absorbed or escapes.

A 23-group neutron cross section library for use with the MORSE code was produced using SUPERTOG[11] to derive a 100 group (GAM-11 99 groups + 1 thermal group) cross-section set from ENDF/B-IV data files for each material of interest. Data for each material were combined into an ANISN format P-3 library using DLC-2, and this set was further condensed to 23 groups. The group condensations were done assuming a fission spectrum joined by a 1/E distribution to a 300°K Maxwellian.

4.2 The Experimental Simulation

The CRNL version of the NMTC code can only accommodate cylindrical geometry, and, although the detailed geometry of the beam tube, target tube, target can, and target was represented exactly, the water bath had to be approximated in the NMTC calculation by a concentric cylinder of length 152.4 cm and radius 85.73 cm.

In MORSE calculations the same horizontal beam tube, target tube, target can, and target were represented but the experimental vertical water bath orientation was treated explicitly as a cylinder of 152.4 cm diameter and 171.45 cm height. In both calculations the aluminum tank was ignored.

In order to determine a calculated flux distribution the water bath was split into zones for the MORSE calculations, the mesh chosen being a compromise between providing large enough regions for acceptable statistical accuracy and yet small enough to enable the flux variation to be reasonably defined.

4.3 Results and Comparisons

The calculated neutron yields are shown in Table 1. Agreement with the measured value is good for the lead target but not for the lithium. This is perhaps not surprising since NMTC was designed for targets of heavy nuclei and for proton beams of energy >100 MeV.

To compare the measured fluxes with those from MORSE it was necessary to integrate the measured distribution over the large zones used in the calculation. The same integration method as for the yield calculation was used. For the lead target axial distributions are compared in Fig. 5 and radial in Fig. 6. Normalization is to the same proton current and agreement is generally good. The error bars represent the statistical errors of the Monte Carlo calculation. Similar results for the lithium target are shown in Figs. 7 and 8. Here the agreement is not good; even if the difference in neutron yield is removed by renormalization, the calculated fluxes clearly fall off more rapidly than the measured.

5. CONCLUSIONS AND FUTURE PLANS

We have measured the neutron yield from thick targets of Pb and Li-7 irradiated with 100 MeV protons with a precision of about $\pm$6%. The computer code NMTC calculates a neutron yield from the high mass number target which is in satisfactory agreement with the measured value. This is not true of the Li-7 target where the calculated value is some 33% higher than that measured. The combination of codes NMTC and MORSE provide a satisfactory description of the thermal neutron distribution in light water moderator surrounding the Pb target. For the Li-7 target they predict a

more rapid fall off of the flux than is observed. This is consistent with the calculated neutron source spectrum being too soft.

We plan future measurements on both light (Be,D_2O) and heavy (U,Th) target materials. It is also expected that we will measure yields from accelerator structural materials such as the medium-weight elements Cu and Fe.

6. REFERENCES

1. G.A. Bartholomew, Research Opportunities with Prototype Accelerators for an Accelerator Breeder, Proc. ICANS-V, Julich, June 1981.

2. J.S. Fraser et al., A Review of Prospects for an Accelerator Breeder, Atomic Energy of Canada Limited, Report AECL-7260, 1981.

3. C.H. Westcott et al., Effective Cross Sections and Cadmium Ratios for the Neutron Spectra of Thermal Reactors, Atomic Energy of Canada Limited, Report AECL-612, 1958.

4. G.M. Roe, The Absorption of Neutrons in Doppler Resonances, KAPL-1241, (1954).

5. C.B. Bigham et al., Experimental Effective Fission Cross Sections and Neutron Spectra on a Uranium Fuel Rod, Part II, Atomic Energy of Canada Limited, Report AECL-1350, 1961.

6. W.A. Coleman and T.W. Armstrong, The Nucleon-Meson Transport Code NMTC, ORNL-4606, 1970.

7. H.W. Bertini, Intranuclear-Cascade Calculation of the Secondary Nuclear Spectra from Nuclear-Nucleus Interactions in the Energy Range 340 to 2900 MeV and Comparison with Experiment, Phys. Rev. 188, 1711, 1969.

8. M.P. Guthrie, EVAP-4: Another Modification of a Code to Calculate Particle Evaporation from Excited Compound Nuclei, ORNL-TM-3119, 1970.

9. E.A. Straker, P.N. Stevens, D.C. Irving and V.R. Cain, The MORSE Code - A Multigroup Neutron and Gamma-Ray Monte Carlo Transport Code, ORNL-4585, 1970.

10. E.A. Straker, W.H. Scott Jr. and N.R. Byrn, The MORSE Code with Combinatorial Geometry, DNA-2860 T, 1972.

11. R.Q. Wright, N.M. Greene, J.L. Lucius and C.W. Craven Jr. SUPERTOG: A program to Generate Fine Group Constants and Pn Scattering Matrices from ENDF/B, ORNL-TM-2679, Rev. 1973.

TABLE 1

Measured and Calculated Neutron Yields

Target Material	Au Foil Thickness Used (mm)	Measured Yield (n/p)	Calculated Yield (n/p)
Pb	0.254	0.330	0.363 ± 0.002
"	0.254	0.346	
"	0.051	0.353	
Li-7	0.254	0.123	0.160 ± 0.001

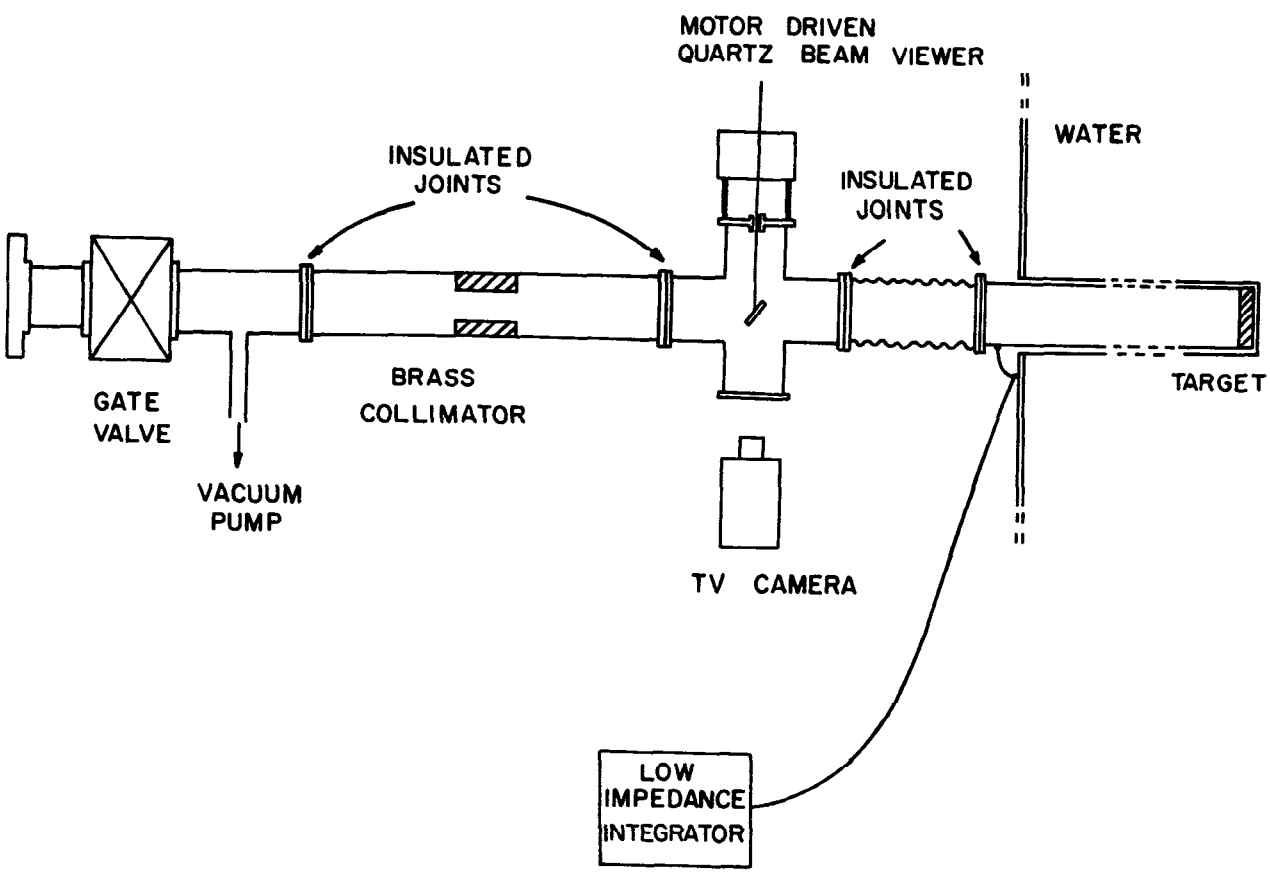

Fig. 1: Beam Line and Target Arrangement

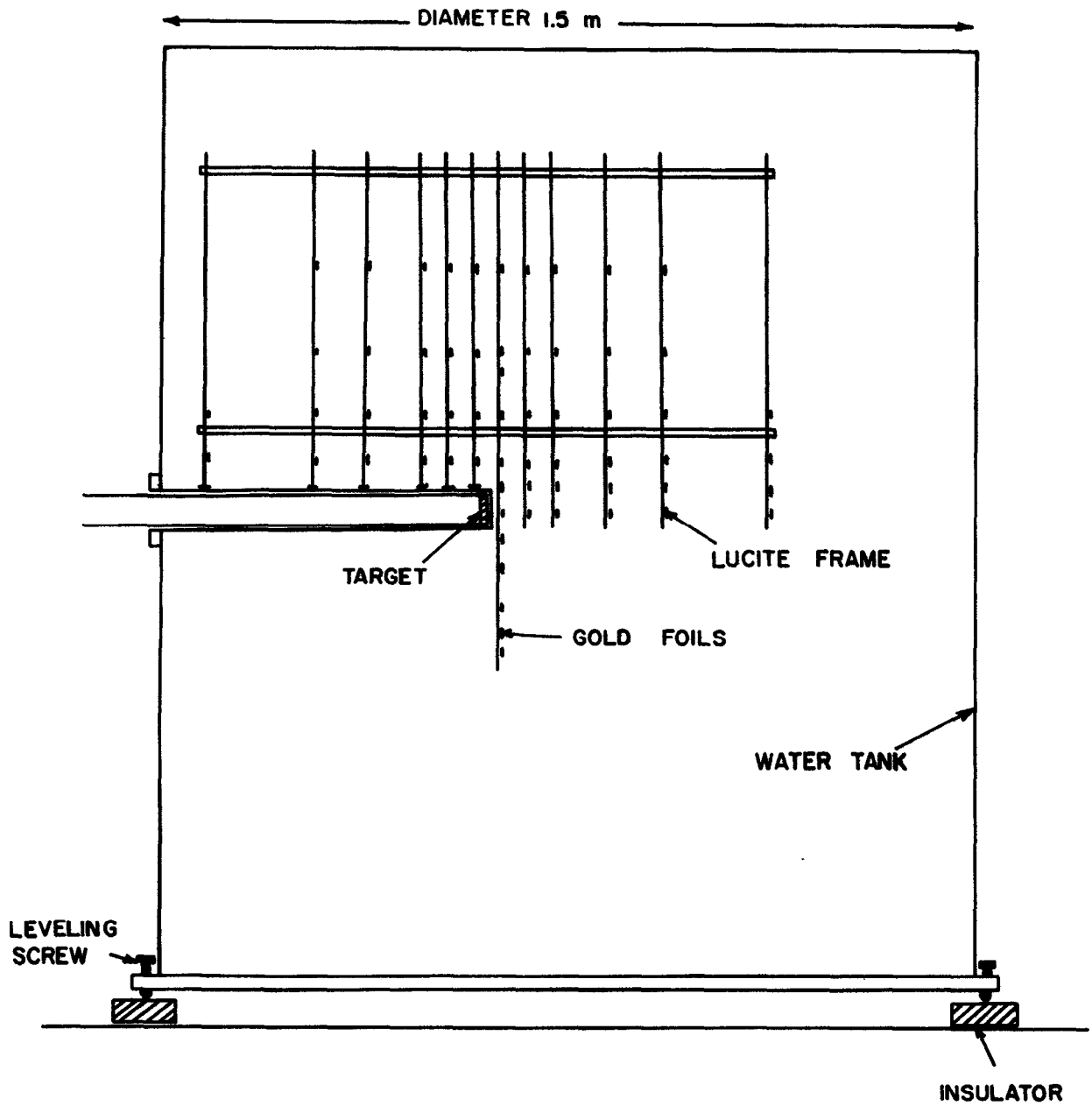

Fig. 2: Water Tank and Foil Array

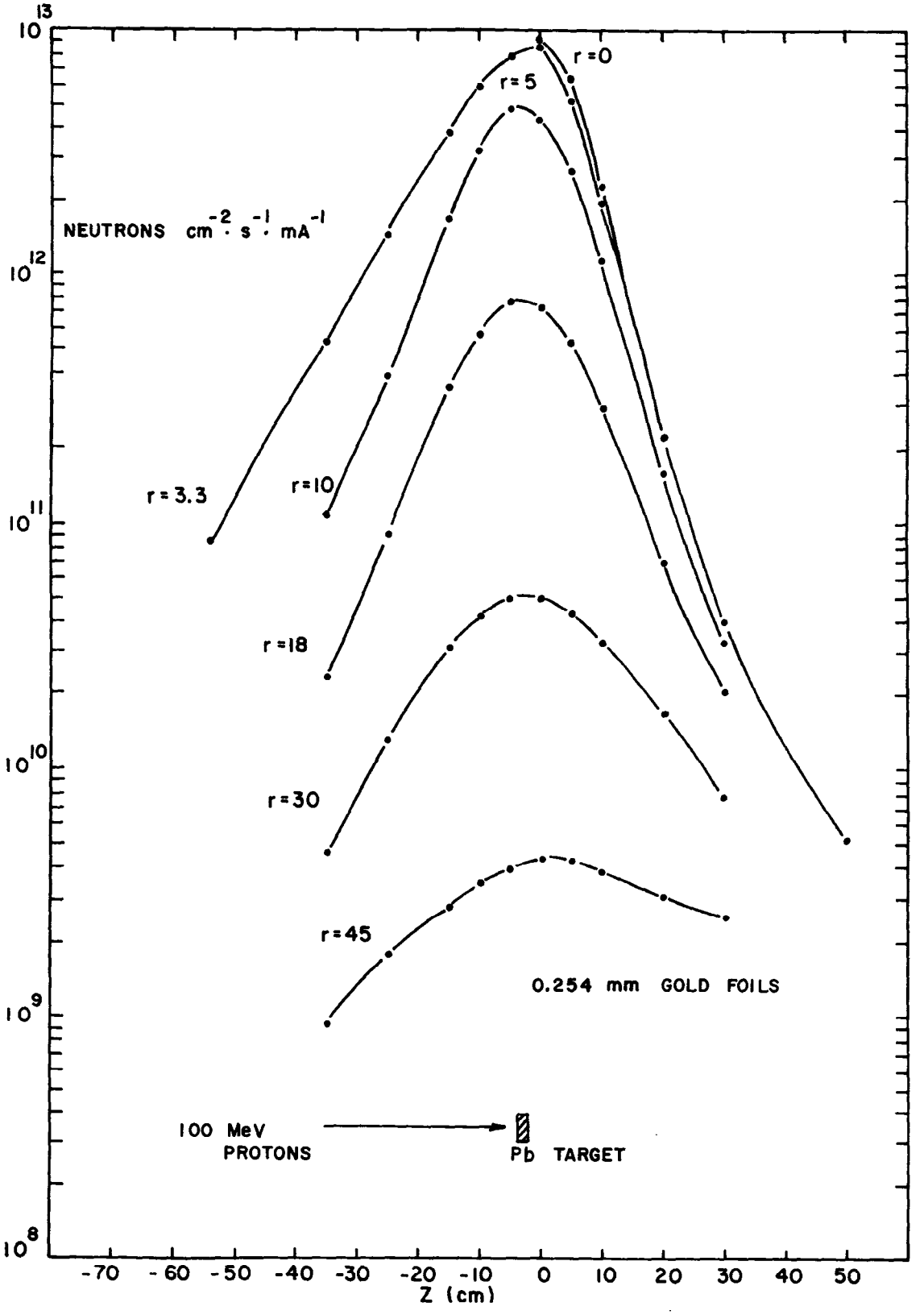

Fig. 3: Thermal Neutron Flux Distribution (Pb Target)

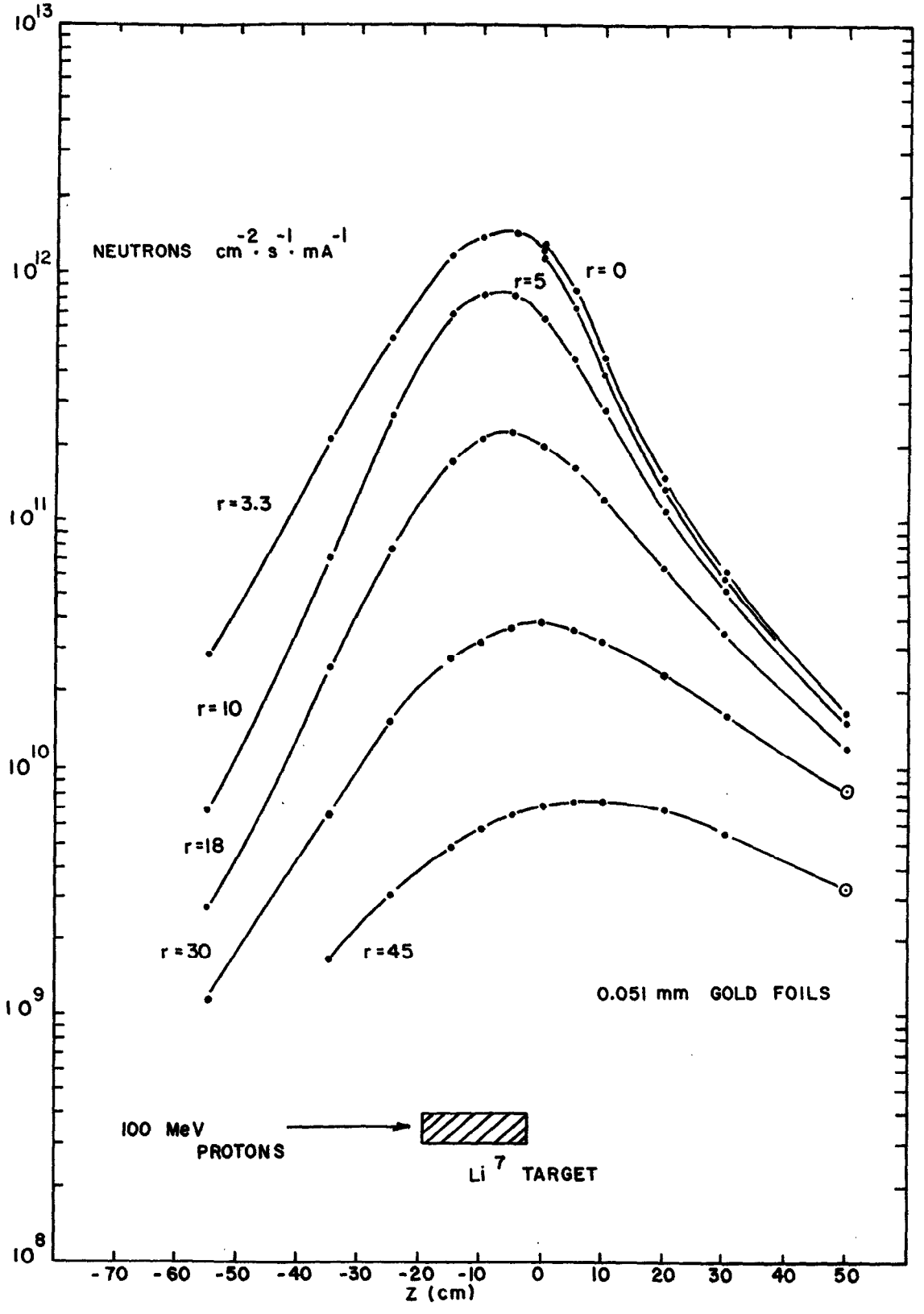

Fig. 4: Thermal Neutron Flux Distribution (Li-7 Target)

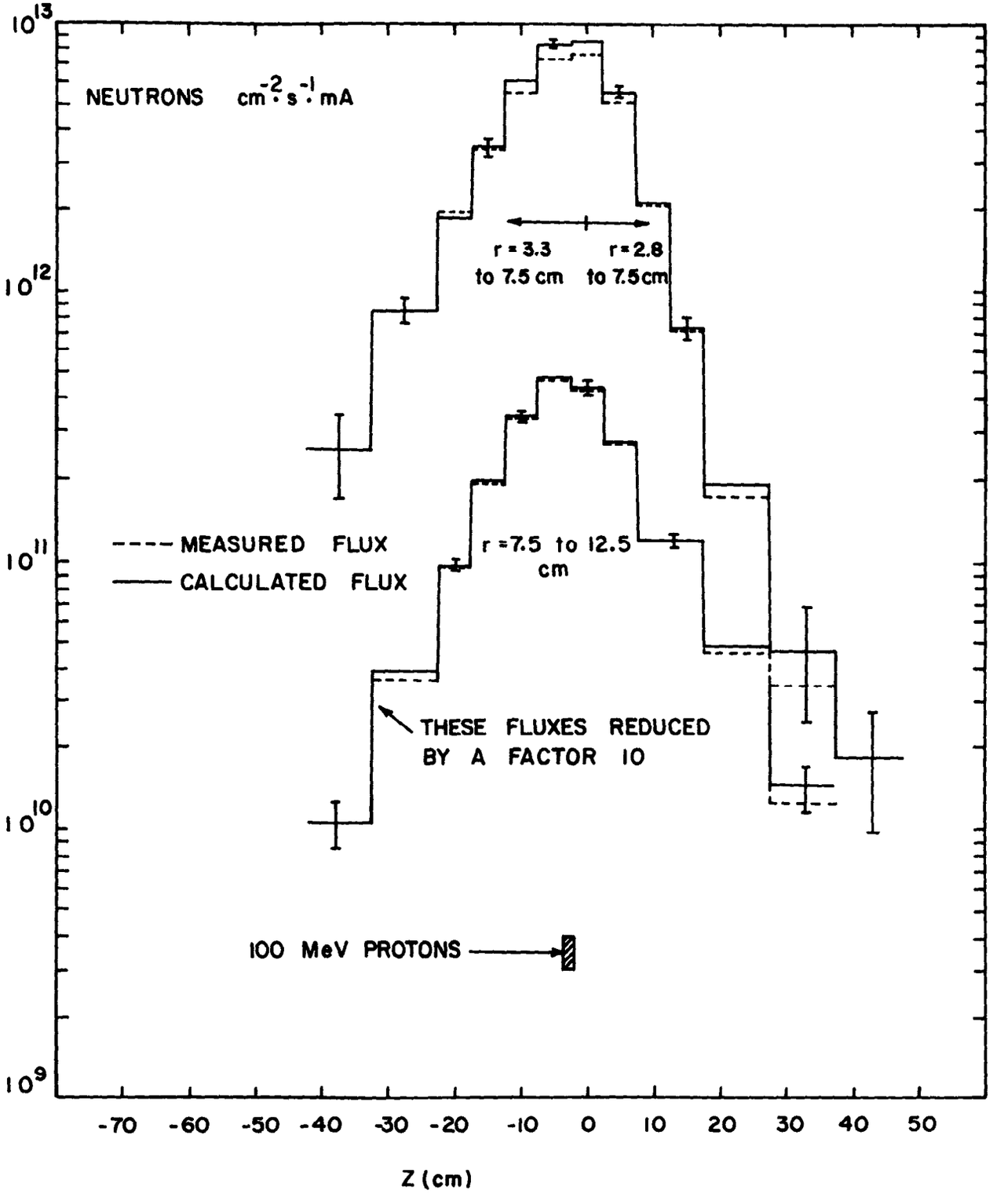

Fig. 5: Comparison of Axial Flux Distributions (Pb Target)

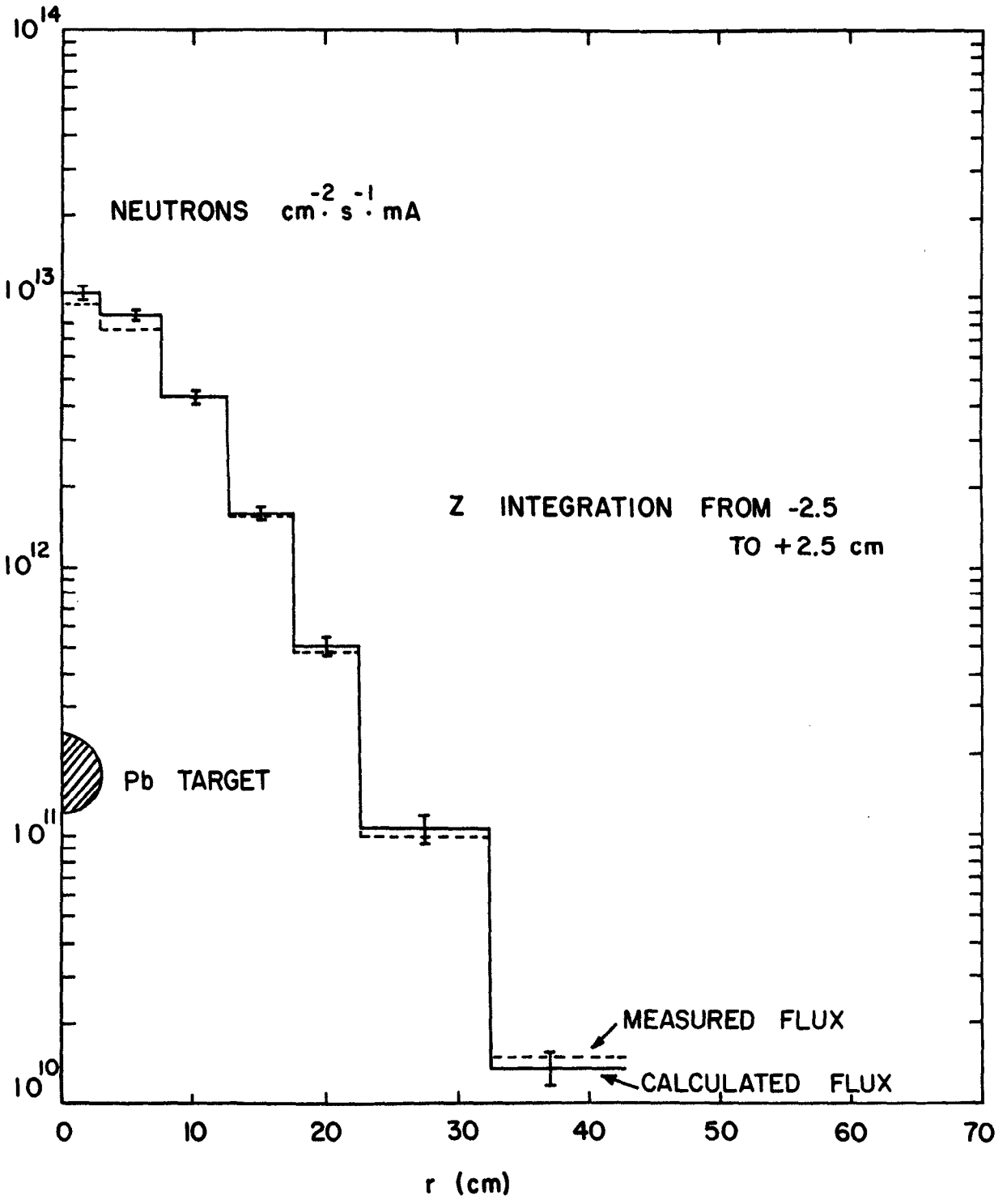

Fig. 6: Comparison of Radial Flux Distributions (Pb Target)

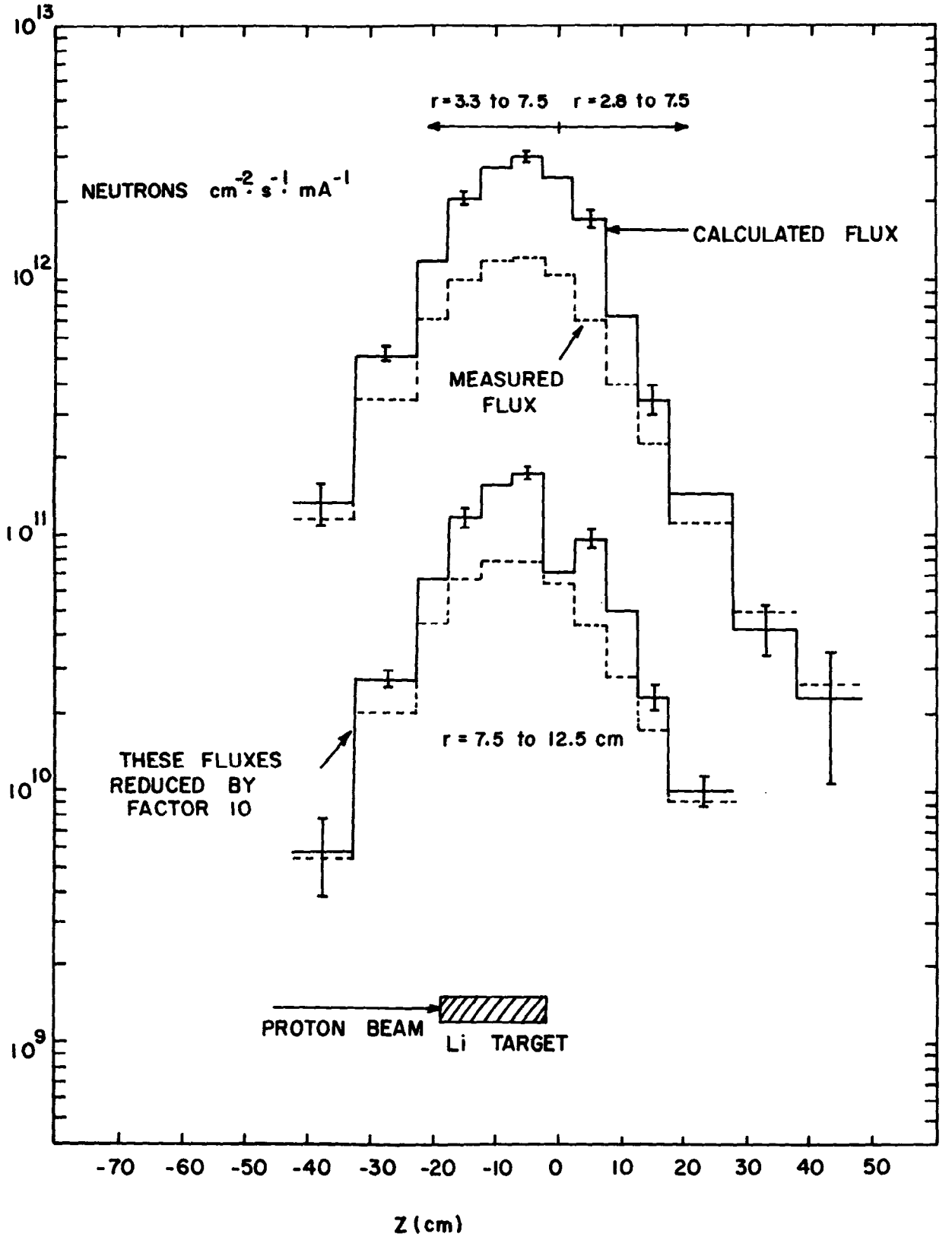

Fig. 7: Comparison of Axial Flux Distributions (Li-7 Target)

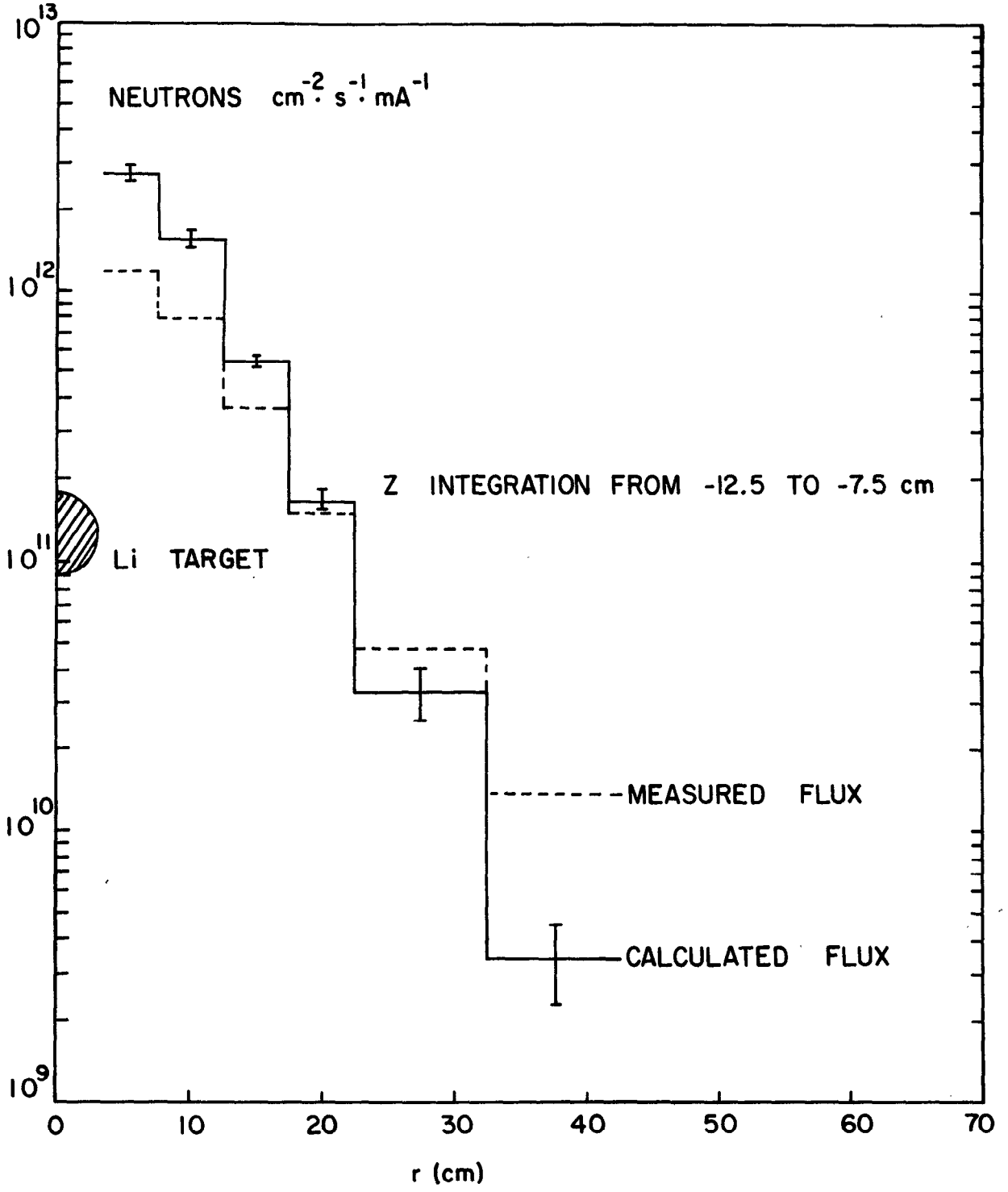

Fig. 8: Comparison of Radial Flux Distributions (Li-7 Target)